Dalton Transactions

Accepted Manuscript

ROYAL SOCIETY OF CHEMISTRY

www.rsc.org/dalton

Journal Name

ARTICLE

Hydrothermal Synthesis and Structural Characterization of Metal–Organic Frameworks Based on New Tetradentate Ligands

Received 00th January 20xx,
Accepted 00th January 20xx

DOI: 10.1039/x0xx00000x

www.rsc.org/

Yue Liang, Wei-Guan Yuan, Shu-Fang Zhang, Zhan He, Junru Xue, Xia Zhang, Lin-Hai Jing, Da-Bin Qin*

The hydrothermal reaction of two new tetradentate ligands with different metal salts of cadmium nitrate, zinc chloride, cobalt nitrate and deprotonated terephthalic acid (H_2tp), isophthalic acid (H_2ip), 4,4'-oxybisbenzoic acid (H_2obba) in H_2O/DMF or H_2O/methanol gave three metal–organic frameworks (MOFs): $\{[Zn_2(L1)(tp)(formate)_2]\cdot H_2O\}_n$ (**1**), $\{[Cd_2(L2)(ip)_2]\cdot 2H_2O\}_n$ (**2**), $\{[Co_2(L2)(obba)_2]\}_n$ (**3**) (L1 = 1,2-bis {2,6-bis [(1H-imidazol-1-yl) methyl]-4-methylphenoxy} ethane, = 1,3-bis {2,6-bis [(1H-imidazol-1-yl) methyl]-4-methylphenoxy} propane). The structures of the compounds are established by single-crystal X-ray diffraction. Compound **1** is a three-dimensional (3D) framework with 2-fold interpenetrated form, which exhibits a 2-nodal (3,4)-connected **fsh**-3,4-*P2₁/c* net with a $\{8^3\}_2\{8^5.10\}$ topology. Complex **2** shows a 2-nodal 4,8-connected 3D framework, the dinuclear cadmium clusters secondary building unit (SBU) assembles with isophthalate and ligand L2 to construct a rare topological type of **sqc22** net with a $\{3^2.5^4\}\{3^4.4^4.5^{10}.6^{10}\}$ topology. Whereas, complex **3** can be extended to a 2D interlocked (4,4)-connected **4,4 L28** net with the point symbol of $\{4.6^4.8\}_2\{4^2.6^4\}$. L1 and L2 are tetradentate ligand with diverse linker and display different coordination modes. In addition, the thermal stability and photochemical properties of the complexes are also investigated.

Introduction

Metal–organic frameworks (MOFs) containing different metal ions or clusters and organic ligands have a variety of intriguing structures and potential applications, such as catalysis, gas storage, adsorption, magnetism, luminescence and so on.[1] In recent years, the design and synthesis of MOFs have been a main stream of active research.[2] However, it is still a great challenge for chemists to develop efficient synthetic strategies to generate MOFs with expected structures and properties. In theory, many variables such as organic ligands, solvent systems, metal ions, flexibility, temperature and counterions are found to influence the construction of molecular architectures during the self-assembly process, but a lot of compounds are achieved by effectively controlling these conditions, for example, MOF-5, MOF-177, MOF-180, MOF-200 and a series of isoreticular MOFs (IRMOFs) with exceptional porosities were obtained by increasing the length or the organic ligands.[3] All in all, the characteristic of the primary organic ligands and the metal centers are more important than other factors to decide the properties and potential applications of the frameworks.[4]

According to study, rigid ligands have the advantage of predicting special topologies in the design strategy,[5] However, MOFs with flexible ligands exhibit more complicated and novel architectures because coordinating groups could freely rotate to meet the metal ions in the assembly process.[6] Therefore, the synthesis of a novel organic primary ligand with flexible chain and rigid functional groups is an interesting direction to construct three-dimensional metal-organic frameworks possessing fascinating topologies and properties.[7]

In this spirit, we use the alkyl chain as a flexible linker that connects two rigid benzene rings, in which bear two imidazole functional groups, and synthesize two new flexible ligands, namely: 1,2-bis{2,6-bis[(1H-imidazol-1-yl) methyl]-4-methylphenoxy} ethane (L1), 1,3-bis{2,6-bis[(1H-imidazol-1-yl) methyl]-4-methylphenoxy} propane (L2) (Scheme 1). In the two ligands, the rigid benzene ring and the flexible -O-$(CH_2)_n$-O- coexist, which can limit freedom of rotation and decrease influence factors on self-assembly. Up to now, a lot of bidentate or tridentate N-containing ligands in metal-polycarboxylate systems have been reported,[8] however, the research of multidentate N-containing ligands is still less reported.[9] Moreover, tetradentate ligands often as 4-connected nodes in the framework of topological type, which is conducive to form novel 4-

[a] *Key Laboratory of Chemical Synthesis and Pollution Control of Sichuan Province, School of Chemistry and Chemical Engineering, China West Normal University, Nanchong 637002, P. R. China.*
† Fax: +86-817-2568081;Tel: +86-817-2568081; E-mail: qdbkyl@cwnu.edu.cn
Electronic Supplementary Information (ESI) available: Experimental details; crystal data, additional figures, TGA, XRPD, NMR spectras, FT-IR spectra, SEM, TEM , Luminescence spectra , Melting points, Elemental analyses.

connected topologies.

Scheme 1. Two Novel Tetradentate Imidazole Ligands and Carboxylate Ligands

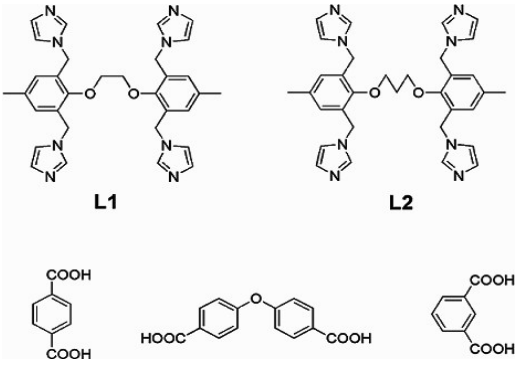

In the present work, we report the syntheses, crystal structures, and properties of three metal–organic frameworks (MOFs): {[Zn_2(L1)(tp)(formate)$_2$]·H_2O}n (**1**), {[Cd_2(L2)(ip)$_2$]·$2H_2O$}n (**2**), {[Co_2(L2)(obba)$_2$]}n (**3**) based on two new quadridentate imidazole ligands L1 and L2 (L1 = 1,2-bis {2,6-bis [(1H-imidazol-1-yl) methyl]-4-methylphenoxy} ethane, L2 = 1,3-bis {2,6-bis [(1H-imidazol-1-yl) methyl]-4-methylphenoxy} propane), which are characterized by single-crystal X-ray diffraction analyses, PXRD, IR spectroscopy, thermogravimetric and photoluminescent analyses.

Experimental section

Materials and Methods

All chemicals were commercially available and used without any further purification. Two new ligands 1,2-bis {2,6-bis [(1H-imidazol-1-yl) methyl]-4-methylphenoxy} ethane (L1), 1,3-bis {2,6-bis [(1H-imidazol-1-yl) methyl]-4-methylphenoxy} propane (L2) were prepared according to the literature.[10] NMR spectra were recorded on an advance Ш 400 Bruker (^{1}H, 400 MHz; ^{13}C, 100 MHz, respectively). FT-IR spectra were recorded on a Nicolet 6700 using KBr disk in the region of 400-4000 cm^{-1}. Powder X-ray diffraction (PXRD) patterns were measured on Dmax/Ultima IV. Thermogravimetric analysis (TGA) were performed on a Netzsch STA 449 F3 from room temperature to 800 °C at a heating rate of 10 °C·min^{-1} in a N_2 atmosphere. Melting points were measured on a XRC-1 micro-melting point apparatus. Elemental analyses (C, H, N) was performed on a Perkin-Elmer 240 elemental analyzer. Scanning Electron Microscope (SEM) images analyses were taken by FEI Quanta 600 FE-SEM. Transmission electron microscope (TEM) images analyses were investigated by FEI Tecnai G2 20 STWIN. Luminescence spectra for the solid samples were recorded on an AMINCO Bowman Series 2 fluorescence spectrophotometer. The raman spectra were measured by rainie salt inVia Reflex laser microscopic confocal Raman spectrometer.

Synthesis of the Ligand L1. Imidazole (0.58 g, 9 mmol) and sodium hydride (0.43 g, 20 mmol) were refluxed with stirring in tetrahydrofuran (12 ml) for 1 h under N_2 atmosphere. Over a period of 5h, 1,2-bis[2,6-bis (bromine methyl)-4-methylphenoxy] ethane (0.63 g, 1 mmol) in tetrahydrofuran (10 ml) was added dropwise. After a further 48 h, the solution was cooled, distilled water (10 ml) was slowly added and the whole was reduced to dryness at 30 °C under reduced pressure. The residue was purified by silica column chromatography to afford products. Yield: 0.47 g, 83%. m.p. 165-166 °C. Anal. Calcd for $C_{32}H_{34}N_8O_2$: C, 68.31; H, 6.09; N, 19.91. Found: C, 68.29; H, 5.59; N, 19.95. ^{1}H NMR ($CDCl_3$, 400 MHz), δ: 7.53 (s, 4H, N=CH), 7.07 (s, 4H, Ph-H), 6.95 (s, 4H, N-CH), 6.87 (s, 4H, N-CH), 5.11 (s, 8H, N-CH_2), 3.51 (t, 4H, -CH_2), 2.30 (s, 6H, -CH_3). ^{13}C NMR (100 MHz, $CDCl_3$): δ 152.26, 137.48, 135.85, 131.28, 129.70, 119.06, 73.01, 45.84, 20.81 ppm.

Synthesis of the Ligand L2. The L2 was prepared by using the similar process that obtained L1 except that 1,2-bis[2,6-bis (bromine methyl)-4-methylphenoxy] ethane was replaced by 1,3-bis[2,6-bis (bromine methyl)-4-methylphenoxy] propane (0.63 g, 1 mmol), gained the white powder. Yield: 0.46 g, 80%, m.p. 169-170 °C. Anal. Calcd for $C_{33}H_{36}N_8O_4$: C, 68.73; H, 6.29; N, 19.43. Found: C, 68.72; H, 6.20; N, 19.46. ^{1}H NMR ($CDCl_3$, 400 MHz), δ: 7.54 (s, 4H, N=CH), 7.07 (s, 4H, Ph-H), 6.90 (s, 4H, N-CH), 6.84 (s, 4H, N-CH), 5.07 (s, 8H, N-CH_2), 3.60 (t, *J* = 8Hz, 4H, O-CH_2), 2.25 (s, 6H, -CH_3), 2.19 (m, 2H, -CH_2). ^{13}C NMR (100 MHz, $CDCl_3$): δ 152.44, 137.36, 135.50, 130.64, 129.84, 129.50, 119.20, 71.23, 45.73, 31.06, 20.79 ppm.

Synthesis of {[Zn_2 (L1)(tp)(formate)$_2$]·H_2O}$_n$ (1). A mixture of DMF/H_2O (7/4) containing the L1 (57.6 mg, 1 mmol), terephthalic acid (16.7 mg, 1 mmol) and $ZnCl_2$ (54.4 mg, 4 mmol) was placed in a Teflon vessel within the autoclave. The vessel was heated at 160 °C for 96 h and then cooled to room temperature. The large quantities of colorless-block crystals were obtained and crystals were filtered off, washed with quantities of distilled water and dried under ambient conditions. Yield of the reaction was ca. 70% based on L1 ligand. Anal. Calcd for $C_{42}H_{40}N_8O_{11}Zn_2$: C, 52.28; H, 4.35; N, 11.62. Found: C, 52.25; H, 4.13; N, 11.68. IR (cm^{-1}): 3441(s), 3122(m), 2928(w), 2815(w), 1673(m), 1623(s), 1526(m), 1476(m), 1440(s), 1348(s), 1235(m), 1147(m), 1104(m), 1010(w), 953(w), 867(w), 820(w), 750(m), 657(w), 583(w).

Synthesis of {[Cd_2(L2)(ip)$_2$]·$2H_2O$}$_n$ (2). A mixture of methanol/H_2O (12/5) containing the L2 (57.6 mg, 1 mmol), isophthalic acid (16.7 mg, 1 mmol) and $Cd(NO_3)_2$·$6H_2O$ (69.0 mg, 2 mmol) was placed in a Teflon vessel within the autoclave. The vessel was heated at 160 °C for 96 h and then cooled to room temperature. The large quantities of yellow-block crystals were obtained and crystals were filtered off, washed with quantities of distilled water and dried under ambient conditions. Yield was ca. 20% based on L2 ligand. Anal. Calcd for $C_{49}H_{48}N_8O_{12}Cd_2$: C, 50.43; H, 4.17; N, 9.61. Found: C, 50.41; H, 4.08; N, 9.65. IR (cm^{-1}): 3436(s), 3120(m), 2930(m), 1613(s), 1513(s), 1463(s), 1396(m), 1354(m), 1285(m), 1225(m), 1143(m), 1109(s), 1085(s), 1030(m), 974(m), 930(m), 833(w), 740(m), 660(s), 632(w), 582(w).

Synthesis of {[Co_2(L2)(obba)$_2$]}$_n$ (3). A mixture of DMF/H_2O (8/5) containing the L2 (57.6 mg, 1 mmol), 4,4'-oxybisbenzoic acid (25.9 mg, 1 mmol) and $Co(NO_3)_2$·$6H_2O$ (59.0 mg, 2 mmol) was

placed in a Teflon vessel within the autoclave. The vessel was heated at 160 °C for 96 h and then cooled to room temperature. The large quantities of violet-block crystals were obtained and crystals were filtered off, washed with quantities of distilled water and dried under ambient conditions. Yield was ca. 80% based on L2 ligand. Anal. Calcd for $C_{61}H_{52}N_8O_{12}Co_2$: C, 60.69; H, 4.31; N, 9.28. Found: C, 60.67; H, 4.22; N, 9.26. IR (cm^{-1}): 3395(m), 3114(m), 2952(m), 1672(s), 1599(s), 1562(s), 1519(m), 1370(s), 1286(m), 1239(s), 1159(s), 1103(s), 1027(m), 950(m), 877(m), 855(m), 799(m), 660(s), 567(m).

Adsorption of C_{60} in Compound 1. Freshly prepared compound **1** (10 mg) was ground and soaked in $CHCl_3$ solutions of C_{60} (10 ml, 0.10 mmol/L). They were soaked for four days, and then washed with quantities of $CHCl_3$ and dried under ambient conditions. The elemental analyses and the powder X-ray diffraction (PXRD) patterns were examined. The structure and morphology of the materials were characterized by scanning electron microscope (SEM) and transmission electron microscope (TEM) at 200kv.

X-ray Crystallography. The X-ray crystallographic data of **1**, **2** and **3** were collected on Bruker APEX-II CCD diffractometer with graphite monochromatic Mo-Kα diation (λ = 0.71073 Å) using the *ω*-scan technique. The structures were solved by direct methods and all non-hydrogen atoms were refined anisotropically except some free solvent molecules with the full-matrix least-squares procedures on F^2 using the SHELXL-97 program.[11] The hydrogen atom positions were generated geometrically at idealized positions and refined by using the riding model. In the structure of **3**, free solvent molecules such as DMF, water were removed using the SQUEEZE routine of PLATON for highly disordered and then refined again using the data generated.[12] The topological analysis and some diagrams were produced using the TOPOS program.[13] The relevant crystallographic crystal data and corresponding structures refinement parameters for three compounds are summarized in Table 1, the selected bond lengths and angles are listed in Table S1.

Table 1. Crystal Data and Structure Refinement Data for Compounds **1**-**3**

Complexes	1	2	3
Empirical formula	$C_{42}H_{40}N_8O_{11}Zn_2$	$C_{49}H_{48}N_8O_{12}Cd_2$	$C_{61}H_{52}N_8O_{12}Co_2$
Formula weight	963.56	1165.72	1206.97
Crystal system	Monoclinic	Orthorhombic	Triclinic
Space group	$P2_1/c$	$C222_1$	p_1
a/Å	13.053(8)	17.811(8)	14.4417(3)
b/Å	8.067(5)	19.155(8)	23.1157(8)
c/Å	23.754(11)	14.683(6)	25.9453(10)
α/deg	90.00	90.00	114.309(4)
β/deg	117.71(2)	90.00	100.856(3)
γ/deg	90.00	90.00	97.740(2)
V/Å^3	2214(2)	5009(4)	7531.1(4)
T/K	293(2)	296(2)	293(2)
Z	2	4	4
Dcalc/g cm^{-3}	1.445	1.540	1.0645
μ/mm^{-1}	1.151	0.918	0.494
F(000)	992	2344	2496
Reflections collected	11593	13276	63713
Independent reflections	4337	4892	26539
GOF on F^2	1.036	1.036	1.069
R_1, I > σ(I) (all)	0.0402 (3312)	0.0459 (4332)	0.0845(16664)
wR_2, I > σ(I) (all)	0.1088 (4316)	0.1301 (4892)	0.1856(26539)

[a] $R_1 = \Sigma||F_o| - |F_c||/|\Sigma|F_o|$, [b] $wR_2 = [\Sigma w(F_o^2 - F_c^2)^2/\Sigma w(F_o^2)^2]^{1/2}$.

Results and discussion

Crystal Structure of $\{[Zn_2(L1)(tp)(formate)_2]\cdot H_2O\}_n$ (1). Single crystal X-ray analysis revealed that compound **1** crystallizes in the monoclinic crystal system of $P2_1/c$. The asymmetric unit consists of one Zn(II) cation, half L1 ligand molecule, half deprotonated terephthalate anion, one formate anion which comes from the decomposition of DMF solvent molecule and half disordered lattice water molecule. As shown in Figure 1a, each Zn1(II) is four-coordinate with distorted tetrahedral geometry by two N (N1, N3) atoms from two different L1 ligands, a carboxylic O (O1) atom from terephthalate and a carboxylic O (O4) atom from a formate anion. The Zn-O lengths are in the range of 1.96(2) ~ 1.97(3) Å and the Zn-N lengths are 2.01(3) ~ 2.03(3) Å. They are both within the ranges reported for tetrahedral Zn complexes.[14] Especially, an interesting feature in this framework is that four imidazole groups and two benzene groups forming a loop like a metal hybrid calix[6]arene, seeing along the b axis (Figure 1b). The imidazole groups of L1 ligand link four Zn ions and the terephthalate connecting two Zn ions to form a 3D network, resulting in large cavities within the network, the size of the cavity is about 11.001 × 21.834 Å^2 along the b axis (Figure 1c). During the assembly process, the potential voids are large enough to be filled via mutual interpenetration of an independent equivalent framework so as to minimize the cavities and to stabilize the framework, generating a 2-fold interpenetrating 3D architecture (Figure 1d). The application of a topological approach by reducing multidimensional structures to simple node and connective nets can better see the nature of this intricate framework.

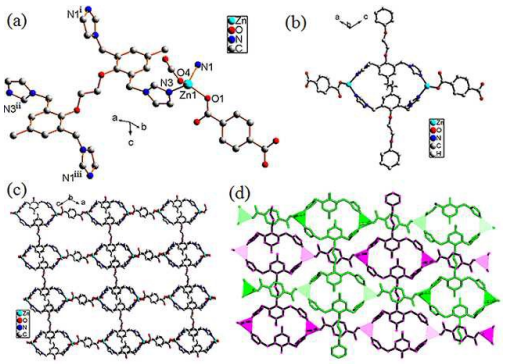

Fig. 1 (a) Coordination environment of the Zn(II) ions in **1**. The hydrogen atoms are omitted for clarity. Symmetry codes: i = 1-x, 0.5+y, 1.5-z; ii = 2-x, 2-y, 2-z; iii = 1+x, 1.5-y, 0.5+z. (b) views of the metal hybrid calix[6]arene-like , seeing along the *b* axis; (c) A view of the 3D network by L1 ligands, terephthalic acid anions and Zn ions along the *b* axis; (d) View of 2-fold interpenetrating 3D packing diagram with polyhedron mode.

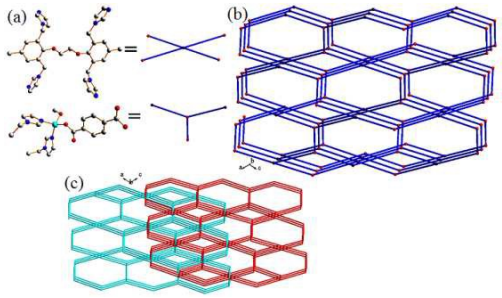

Fig. 2 (a) View of the L1 ligand is simplified to a 4-connecting node and the Zn second building unit is simplified to a 3-connecting node; (b) a 3D component of Zn-L1 sbu net of **1** along the *b* axis; (c) Schematic view of two interpenetrating framework with **fsh**-3,4-$P2_1/c$ topology.

The L1 links four Zn(II) ions and it can be considered as a 4-connected node with a *Schälfli* symbol of $\{8^5.10\}$.[15] We can define Zn(II) as a 3-connected node with a *Schälfli* symbol of $\{8^3\}$ (Figure 2a), which bonds with two L1 ligand and one chelating carboxylate group of terephthalate. Therefore, the whole structure can be represented as a 2-nodal (3,4)-connected **fsh**-3,4-$P2_1/c$ net with a $\{8^3\}_2\{8^5.10\}$ topology (Figure 2b, 2c).[16]

Crystal Structure of $\{[Cd_2(L2)(ip)_2]\cdot 2H_2O\}_n$ (2). Compound **2** crystallizes in the orthorhombic crystal system with space group $C222_1$. The asymmetric unit contains two Cd(II) cations, one L2 molecule, one deprotonated isophthalate anion and two lattice water molecules. As shown in Figure 3a, Cd(II) is seven-coordinated by five oxygen (O2, O3, O4, O5) atoms of bridging carboxylate groups in the equatorial plane and two nitrogen (N1, N4) atoms from two L2 ligands at the axial position resulting in a distorted pentagonal bipyramid coordination geometry. The bond lengths of Cd-O and Cd-N are in the range of 2.41(4) ~ 2.61(4) Å and 2.24(4) ~ 2.24(5) Å.[17] In complex **2**, the crystallographically independent isophthalic acid ligand is completely deprotonated and connects three Cd atoms, moreover, the oxygen atoms from carboxylate groups adopt two kinds of coordination modes. One kind of oxygen atom (O4) as a bridge connects two Cd atoms forming a binuclear clusters unit (Cd1-O4-Cd1-O4), and the distance of Cd(1)···Cd(1) is 3.96(1) Å. The other kind of oxygen atom as a μ-bridge links two binuclear Cd clusters units and each binuclear Cd cluster coordinates to four isophthalate anions to form a 2D layered network (Figure 3b), the size of this net is 7.039 × 14.625 $Å^2$. Furthermore, between the two 2D layered networks, the propagation of accessible distortion of quadrilateral shaped pores is along the *b* axis in which lattice water molecules (O1W) are sitting inside (Figure 3c).[18] Because the water molecule is a litter disordered and whose share is 50%, The hydrogen atoms cannot be obtained by Fourier differential peak synthesis. The L2 ligands linking binuclear Cd clusters in the axial position of the coordination pentagonal bipyramid further generate an infinite 3D framework (Figure 3d, 3e). To analyze the overall topology of complex **2**, the chelating bridge L2 links four Cd(II) ions and it can be considered as a 4-connected node with a *Schälfli* symbol of $\{3^2.5^4\}$. The binuclear clusters unit connects eight oxygen atoms from four crystallographical independent isophthalate and four imidazole groups from L2 ligands and it can be considered as a 8-connected node with a *Schälfli* symbol of $\{3^4.4^4.5^{10}.6^{10}\}$ (Figure 4a). Topological analysis using *TOPOS* software indicates that complex **2** displays a 2-nodal **sqc22** net with a $\{3^2.5^4\}\{3^4.4^4.5^{10}.6^{10}\}$ topology (Figure 4b, 4c). There have been less (4,8)-connected MOFs reported and they are almost concerned with **flu**, **scu**, **alb** and **sqc** nets.[19] As far as we know, compound **2** represents the first MOFs with a (4,8)-connected **sqc22** net.

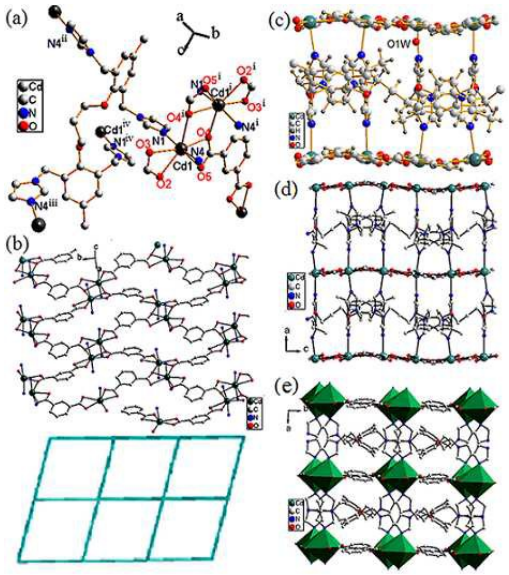

Fig. 3 (a) Coordination environment of the Cd(II) ions in **2**. The hydrogen atoms are omitted for clarity. Symmetry codes: i = x, 2-y, 1-z; ii = 0.5+x, 1.5-y, 1-z; iii = 0.5-x, 1.5-y, 0.5+z; iv = 1-x, y, 1.5-z. (b) views of the 2D network by isophthalic acid and Cd anions; (c) views of the isolated lattice water molecule in the pores along the *b* axis; (d) views of 3D framework of **2** along the *b* axis; (e) views of the 3D packing diagram with polyhedron mode.

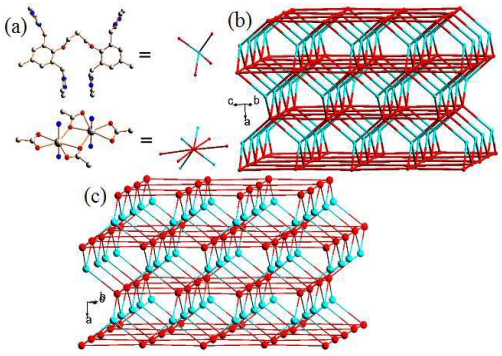

Fig. 4 (a) View of the L2 ligand is simplified to a 4-connecting node and the Cd cluster second building unit is simplified to a 8-connecting node; (b) a perspective of 3D framework in **2**; (c) schematic illustrating the **sqc22** topology of complex **2** (sapphire nodes, Cd(II)-SBU; red, L2).

Crystal Structure of $\{[Co_2(L2)(obba)_2]\}_n$ (3). Compound **3** crystallizes in the triclinic *p_1* space group. The asymmetric unit consists of two Co(II) cations, a L2 ligand molecule, two deprotonated 4,4'-oxybisbenzoic acid anions. As shown in Figure 5a and 5d, each Co1(II) is four-coordinate with distorted tetrahedral geometry by two N (N1, N8) atoms from two different L2 ligands, two carboxylic O (O1, O11) atoms from diverse 4,4'-oxybisbenzoic acid anion. The Co-O lengths are in the range of 1.96(4) ~ 1.99(4) Å and the Co-N lengths are 2.00(5) ~ 2.04(4) Å. They are both within the ranges reported for tetrahedral Co complexes.[20] The imidazole groups of L2 ligand link four Co ions and 4,4'-oxybisbenzoic acid anion connecting two Co ions to form a 2D→2D interlocking network. Especially, unlike compound **1**, a metal hybrid calix[6]arene is formed by four imidazole groups and two benzene groups connecting the cobalt ions (Figure 5b). There are three planes with connection, in which the middle plane extend along the *b* axis of *ab* flat, however, the other two planes similarly stretch along the *a* axis of *ab* flat (Figure 5c, 5d). Through the analysis of topology, the chelating bridge L2 links four Co(II) ions and it can be considered as a 4-connected node with a *Schälfli* symbol of $\{4^2.6^4\}$. We can define Co(II) as a 4-connected node with a *Schälfli* symbol of $\{4.6^4.8\}$ (Figure 6a), which bonds with two L2 ligand and two chelating carboxylate groups of 4,4'-oxybisbenzoic acid, Therefore, the three planes are the same point symbol for net: $\{4.6^4.8\}_2\{4^2.6^4\}$ and the whole structure can be extended to a 2D interlocked (4,4)-connected **4**, **4 L28** net with the point symbol of $\{4.6^4.8\}_2\{4^2.6^4\}$ (Figure 6b, 6c).

Effect of armoatic carboxylates on the structures of the MOFs: In this work, we selected two flexible ligands L1, L2, the rigid terephthalic acid (H_2tp), isophthalic acid (H_2ip) and the flexible 4,4'-oxybisbenzoic acid (H_2obba) to synthesis three novel metal–organic frameworks **1**, **2** and **3,** aiming at examining the effect of aromatic carboxylates. In **1**, **2** and **3**, the flexible L1, L2 have the same coordination mode connecting four divalent metal ions. The tp^{2-} and the $obba^{2-}$ ligands as linker connect adjacent two

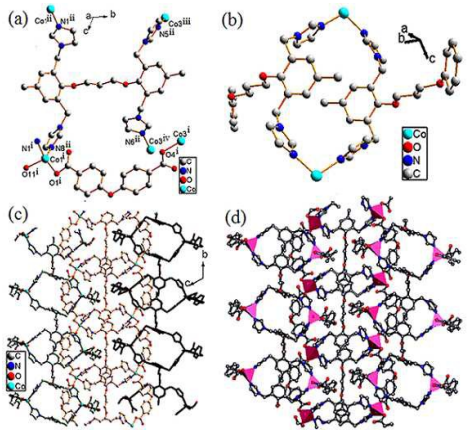

Fig. 5 (a) Coordination environment of the Co(II) ions in **3**. The hydrogen atoms are omitted for clarity. Symmetry codes: i = 1-x, 2-y, 1-z; ii = 1+x, y, z; iii = 1+x, -1+y, z; iv = -x, 2-y, 1-z. (b) view of the metal hybrid calix[6]arene; (c) a view of the 2D network by L2 ligands, 4,4'-oxybisbenzoic acid anions and Co ions along the a axis; (d) view of 2D interlocked packing diagram with polyhedron mode.

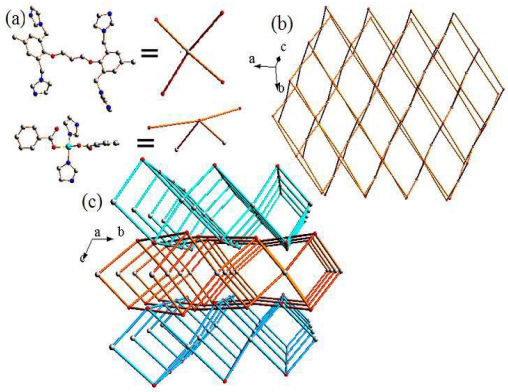

Fig. 6 (a) View of the L2 ligand is simplified to a 4-connecting node and the Co second building unit is simplified to a 4-connecting node; (b) a 2D component of Co-L1 sub net of **3** along the ab plane; (c) schematic view of 2D→2D interlocking framework with **4**,**4 L28** topology.

divalent metal ions form a 3D 2-fold interpenetrating (3,4)-connected **fsh**-3,4-$P2_1/c$ net for **1,** 2D interlocked (4,4)-connected **4**, **4 L28** net for **3,** respectively. For **2,** the ip^{2-} ligands bridge two Cd atoms forming a binuclear cluster and μ-bridge two binuclear Cd clusters units which leads to 3D 2-nodal (4,8)-connected **sqc22** net. The aromatic carboxylates spacers exhibit different bending and rotating ability, which leads to different framworks. In **1** and **2,** the rigid terephthalic acid (H_2tp) and isophthalic acid (H_2ip) conducive to form a stable 3D structure, however, the flexible 4,4'-oxybisbenzoic acid would prefer to form a 2D interlocked consturtion. It can be observed that the different aromatic carboxylates have a great influence on the architecture of frameworks.[21]

Thermal Analysis and PXRD Patterns: Complexes **1**, **2** and **3** are air-stable and insoluble in water and common organic solvents such as methanol, DMF and chloroform. The thermogravimetric analysis (TGA) of compounds **1**, **2** and **3** were carried out to

investigate their thermal stabilities,[22] as shown in Figure 7. Complex **1** shows that it is stable up to 316 °C and then the overall framework begins to collapse. For compound **2**, until 236 °C with the weight loss of 3% corresponding to the release of two lattice water molecules (theoretical 2.76%) then decomposes at 316 °C. Compound **3** displays a high thermal stability**,** the weight loss of 15.64% (theoretical 15.34%) from 25 °C to 343 °C, corresponding to the release of disordered lattice water molecules and DMF molecules, then decomposes at 344 °C.

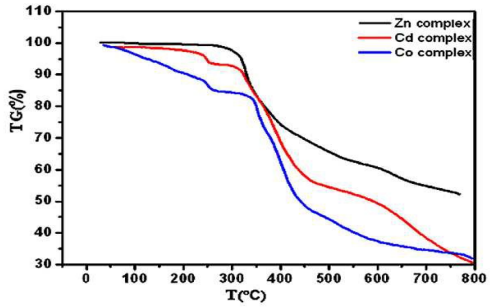

Fig. 7 TGA plots of complexes **1**, **2** and **3**

In order to confirm the phase purity of compounds **1**, **2** and **3**, the powder X-ray diffraction (PXRD) patterns were carried out. Their peak positions were found comparable to the corresponding simulated results from the single-crystal diffraction, indicating the phase purity of bulk synthesized materials (Figure S10, S11 and S12). The crystals were soaked in chloroform ($CHCl_3$) solution two times for 24 h at a time and then dried under vacuum at 100°C. The powder X-ray diffraction pattern and FT-IR spectra of the vacuum-dried samples of **1** showed that the structure still retained (Figure S13 and S14).

Photochemical Properties and Adsorption Performance. For MOFs constructed from d^{10} metal ions and conjugated organic molecules usually exhibit luminescent properties, they are considered as promising candidates for potential photoactive materials.[23] Thus, the photoluminescence (PL) spectra of complexes **1**, **2** in the solid state were studied at room temperature, as depicted in Figure 8. Complex **1** exhibits an intense emission peak with a maximum at 378 nm upon excitation at 300 nm. To understand the nature of the emission spectra, the luminescence properties of the free L1 ligand and the terephthalic acid under the same experimental conditions were recorded for comparison. A weak emission of the L1 ligand is observed with wavelength from 325 to 550 nm (λ_{max} = 389 nm upon excitation at 300 nm), Intense emission of the free terephthalic acid is observed with wavelength of 320 to 470 nm (λ_{max} = 387 nm). The emission peaks of **1** are similar to L1 and terephthalic acid, which indicates that the emission band of **1** may be ascribed to intraligand π-π* or n-π* transitions (LLCT).[24] On the other hand, the terephthalic acid made major contribution to the photoluminescence.[25] In **2** the emission peak at 424 nm (λ_{ex} = 300 nm), there can be observed a red shift (25 nm) in the emission of **2** (λ_{ex} = 300nm, λ_{max} = 424nm) compared with L2 ligand (λ_{max} = 399 nm upon excitation at 300 nm) and isophthalate acid (λ_{ex} = 262nm, λ_{max} = 350nm), which is probably due to the coordination between ligands (L2 and isophthalate acid) and the metal enhancing the conjugation.[26]

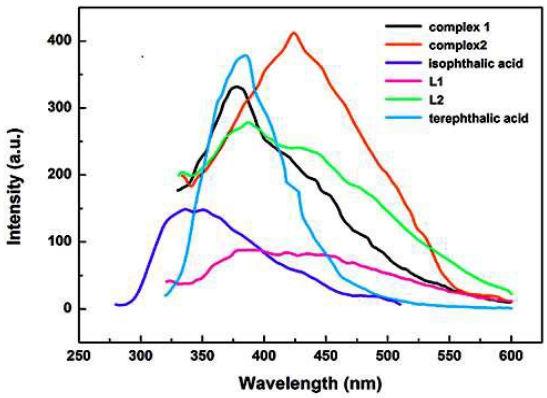

Fig. 8 Photoluminescence spectra of **1**, **2,** L1, L2, isophthalic acid and terephthalic acid in the solid state at room temperature

Complex **1** with a analogues metal hybrid calix[6]arene which contains appropriate pore size (8 ~ 10 Å) and permanent porosity maybe have adsorptivity for C_{60},[27] which was demonstrated in vacuum chamber at 90 °C for 24 h making it suitable as a host for adsorbing C_{60} molecules (the size of 7.1 Å). The compound **1** was introduced into the 0.10 mmol/L C_{60} $CHCl_3$ solution. The colorless crystals gradually turn to faint yellow after three days. Through the comparison of PXRD patterns of complex **1**, C_{60} and soaked complex **1** in C_{60} $CHCl_3$ solution, the main peaks of C_{60} are showed in the PXRD pattern of soaked complex **1** in C_{60} $CHCl_3$ solution (Figure 9a), which demonstrates that C_{60} molecules are adsorbed.[28] In order to further prove this poiont, the element analysis and the raman spectra of soaked complex **1** in C_{60} $CHCl_3$ solution (λ_{ex} = 785 nm) were performed and the characteristic peaks of C_{60} (1468 cm^{-1}) were distinctly observed (Figure S17). Furthermore, the content of carbon element increased (Anal. Calcd: C, 55.69; H, 3.87; N, 10.83). The structure and morphology of the materials were characterized by scanning electron microscope (SEM) (Figure S15) and TEM (Figure S16), which show that the complex **1** have the irregular honeycomb network porous (Figure 9b).[39] The porous crystalline **1** maybe have a good adsorption performance for C_{60} molecule.

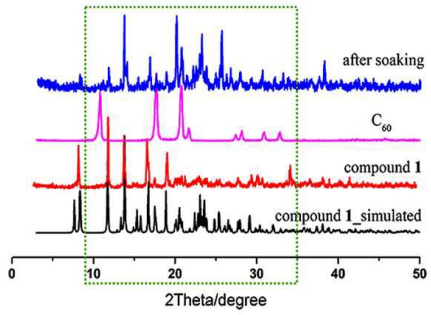

(a)

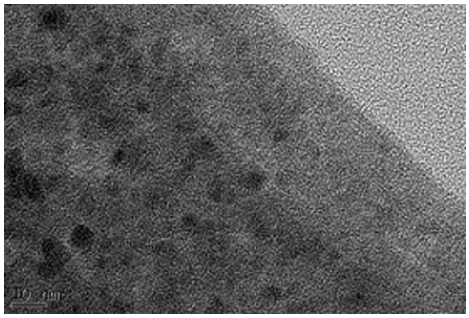

(b)

Figure. 9 (a) The PXRD patterns of soaked compound **1** in 0.1 mmol/L C_{60} $CHCl_3$ solution; (b) high-resolution TEM topograph (10nm) of the irregular honeycomb network **1** was soaked in 0.1 mmol/L C_{60} $CHCl_3$ solution.

Conclusions

In summary, three novel MOFs based on two flexible quadridentate imidazole ligands L1 and L2, have been successfully synthesized and characterized. The results demonstrate that the multidentate imidazole ligand and carboxylate anions play an important role in construction of topological structure. In addition, three complexes display thermal stability, complexes **1**, **2** show strong solid-state fluorescent emission character, which may be good candidates for luminescent materials and compound **1** shows an adsorption property for C_{60} molecule.

Acknowledgments

This work was financially supported by the National Natural Science Foundation of China (21102117), Innovative Research Team in College of Sichuan Province (No. 14TD0016), The Key Laboratory of Chemical Synthesis and Pollution Control of Sichuan Province (CSPC2014-4-1).

References

1 (a) E. K. Brechin, S. G. Harris, A. Harrison, S. Parsons, A. G. Whittaker and R. E. P. Winpenny, *Chem. Commun.*, 1997, 653; (b) M. H. Xie, X. L. Yang and C. D. Wu, *Chem. Commun*., 2011, **47**, 5521; (c) J. R. Li, Y. Ma, M. C. McCarthy, J. Sculley, J. Yu, H. K. Jeong, P. B. Balbuena and H. C. Zhou, *Coord. Chem. Rev*., 2011, **255**, 1791; (d) S. Zheng, T. Wu, C. Chou, A. Fuhr, P. Feng and X. Bu, *J. Am. Chem. Soc.*, 2012, **134**, 4517; (e) K. Wang, D. Feng, T. Liu, J. Su, S. Yuan, Y. Chen, M. Bosch, X. Zou and H. Zhou, *J. Am. Chem. Soc.*, 2014, **136**, 13983; (f) Q. Zhang, J. Su, D. Feng, Z.Wei, X. Zou and H. Zhou, *J. Am. Chem. Soc.*, 2015, **137**, 10064.

2 (a) Z. G. Guo, R. Cao, X. Wang, H. F. Li, W. B. Yuan, G. J. W. Wang, H. H. Wu and J. Li, *J. Am. Chem. Soc.*, 2009, **131**, 6894; (b) Q. Yue, L. Yan, J. Y. Zhang and E. Q. Gao, *Inorg. Chem.*, 2010, **49**, 8647; (c) L. Qin, J. S. Hu, M. D. Zhang, Z. J. Guo and H. G. Zheng, *Chem. Commun*., 2012, **48**, 10757; (d) W. G. Yuan, F. Xiong, H. L. Zhang, W. Tang, S. F. Zhang, H. Zhan, L. H. Jing and D. B. Qin, *CrystEngComm*, 2014, **16**, 7701.

3 (a) O. M. Yaghi, M. O'Keeffe, N. W. Ockwig, H. K. Chae, M. Eddaoudi and J. Kim, *Nature*, 2003, **423**, 705; (b) F. Luo, Y. X. Che and J. M. Zheng, *Cryst. Growth Des*., 2009, **9**, 1066; (c) Y. Q. Tian, Y. M. Zhao, Z. X. Chen, G. N. Zhang, L. H. Weng and D. Y. Zhao, *Chem. Eur. J*.**,** 2007, **13**, 4146; (d) Z. W. Wang, C. C. Ji, J. Li, Z. J. Guo, Y. Z. Li and H. G. Zheng, *Cryst. Growth Des*., 2009, **9**, 475; (e) H. Furukawa, N. Ko, Y. B. Go, N. Aratani, S. B. Choi, E. Choi, A. Ö. Yazaydin, R. Q. Snurr, M. O'Keeffe, J. Kim and O. M. Yaghi, *Science*, 2010, **329**, 424; (f) M. El Garah, N. Marets, M. Mauro, A. Aliprandi, S. Bonacchi, L. De Cola, A. Ciesielski, V. Bulach, M. W. Hosseini and P. Samorì, *J. Am. Chem. Soc.*, 2015, **137**, 8450.

4 F. A. Almeida Paz, J. Klinowski, S. M. F. Vilela, J. P. C. Tomé, J. A. S. Cavaleiroc and Rochaa, *J. Chem. Soc. Rev.*, 2012, **41**, 1088.

5 (a) M. Eddaoudi, J. Kim, N. Rosi, D. Vodak, J. Wachter, M. O'Keeffe and O. M. Yaghi, *Science*, 2002, **295**, 469; (b) X. C. Huang, Y. Y. Lin, J. P. Zhang and X. M. Chen, *Angew. Chem., Int. Ed.*, 2006, **45**, 1557; (c) H. Wang, D. Zhang, D. Sun, Y. Chen, K. Wang, Z. Ni, L. Tian and J. Jiang, *CrystEngComm*, 2010, **12**, 1096; (d) N. B. Shustova, A. F. Cozzolino and M. Dincă, *J. Am. Chem. Soc.*, 2012, **134**, 19596.

6 (a) S. K. Henninger, H. A. Habib and C. Janiak, *J. Am. Chem. Soc*., 2009, **131**, 2776; (b) H. A. Habib, A. Hoffmann, H. A. Hoppe, and C. Janiak, *Dalton Trans*., 2009, 1742; (c) P. Ren, M. L. Liu, J. Zhang, W. Shi, P. Cheng, D. Z. Liao and S. P. Yan, *Daton Trans*., 2008, 4711; (d) Z. Lin, J. Lu, M. Hong and R. Cao, *Chem. Soc. sev.*, 2014, **43**, 5867.

7 (a) H. L. Zhang, B. Zhao, W. G. Yuan, W. Tang, F. Xiong, L. H. Jing and D. B. Qin, *Inorg. Chem. Commun.*, 2013, **35**, 208; (b) R. Chakrabarty, P. S. Mukherjee and P. J. Stang, *Chem. Rev.*, 2011, **111**, 6810; (c) M. O'Keeffe and O. M. Yaghi, *Chem. Rev.*, 2012, **112**, 675.

8 (a) J. S. Hu, L. Qin, M. D. Zhang, X. Q. Yao, Y. Z. Li, Z. J. Guo, H. G. Zheng and Z. L. Xue, *Chem. Commun*., 2012, **48**, 681; (b) P. Metrangolo, F. Meyer, T. Pilati, D. M. Proserpio and G. Resnati, *Chem. Eur. J*., 2007, **13**, 5765; (c) R. Natarajan, G. Savitha, P. Dominiak, K. Wozniak and J. N. Moorthy, *Angew. Chem., Int. Ed*., 2005, **44**, 2115; (d) W. Yuan, F. Xiong, H. Zhang, W. Tang, S. Zhang, Z. He, L. Jing and D. Qin, *CrystEngComm*, 2014, **16**, 7701.

9 (a) P. E. Ryan, C. Lescop, D. Laliberté, T. Hamilton, T. Maris and J. D. Wuest, *Inorg. Chem*., 2009, **48**, 2793; (b) L. Qin, J. S. Hu, M. D. Zhang, Y. Z. Li and H. G. Zheng, *Cryst. Growth Des.*, 2012, **12**, 4911; (c) P. Pachfule, R. Das, P. Poddar and R. Banerjee, *Cryst. Growth Des.*, 2010, **10**, 2475; (d) S. Hasegawa, S. Horike, R. Matsuda, S. Furukawa, K. Mochizuki, Y. Kinoshita and S. Kitagawa, *J. Am. Chem. Soc.*, 2007, **129**, 2607.

10 (a) T. I. Richards, K. Layden, E. E. Warminski, P. J. Milburn and E. Haslam, *J. Chem. Soc. Perkin Trans. 1*,1987,

2765; (b) Q. X. Liu, Z. Q. Yao, X. J. Zhao, A. H. Chen, X. Q. Yang, S. W. Liu and X. G. Wang, *Organometallics*, 2011, **30**, 3732.
11 (a) G. M. Sheldrick, *Acta Crystallogr,* 2008, **A64**, 112; (b) G. M. Sheldrick, *SHELXTL*, Version 6.14, Structure Determination Software Suite, Bruker AXS: Madison, WI, 2003.
12 H. L. Jiang, D. W. Feng, K. C. Wang, Z. Y. Gu, Z. W. Wei, Y. P. Chen and H. C. Zhou, *J. Am. Chem. Soc.*, 2013, **135**, 13934.
13 A. Blatov, A. P. Shevchenko and V. N. Serezhkin, *J. Appl. Crystallogr.*, 2000, **33**, 1193.
14 (a) L. F. Ma, Y. Y. Wang, J. Q. Liu, G. P. Yang, M. Du and L. Y. Wang, *CrystEngComm*, 2009, **11**, 1800; (b) A. Z. Thomas, G. Helmar and D. Eckhard, *Polyhedro*, 1998, **17**, 2199.
15 V. A. Blatov, *IUCr CompComm. Newsletter*, 2006, **7**, 4.
16 Y. Gong, T. Wu and J. H. Lin, *CrystEngComm*, 2012, **14**, 3727.
17 (a) X. Q. Yao, D. P. Cao, J. S. Hu, Y. Z. Li, Z. J. Guo and H. G. Zheng, *Cryst. Growth Des.*, 2011, **11**, 231; (b) J. C. Dai, X. T. Wu, Z. Y. Fu, C. P. Cui, S. M. Hu, W. X. Du, L. M. Wu, H. H. Zhang and R. Q. Sun, *Inorg. Chem*., 2002, **41**, 1391.
18 P. Pachfule, R. Das, P. Poddar and R. Banerjee, *Inorg. Chem*., 2011, **50**, 3855.
19 (a) Y. He, Z. Zhang, S. Xiang, F. R. Fronczek, R. Krishna and B. Chen, *Chem. Eur. J*., 2012, **18**, 613; (b) Y. Q. Lan, H. L. Jiang, S. L. Li and Q. Xu, *Inorg. Chem*., 2012, **51**, 7484; (c) L. Wen, P. Cheng and W. Lin, *Chem. Sci*., 2012, **3**, 2288; (d) H. L. Jiang, Q. P. Lin, T. Akita, B. Liu, H. Ohashi, H. Oji, T. Honma, T. Takei, M. Haruta and Q. Xu, *Chem. Eur. J*.**,** 2011, **17**, 78; (e) H. L. Jiang, D. W. Feng, K. C. Wang, Z. Y. Gu, Z. W. Wei, Y. P. Chen and H. C. Zhou, *J. Am. Chem. Soc.*, 2013, **135**, 13934.
20 (a) Y. G. Huang, D. Q Yuan, L. Pan, F. L. Jiang, M. Y. Wu, X. D. Zhang, W. Q. Gao, J. Y. Lee, J. Li and M. C. Hong, *Inorg. Chem.*, 2007, **46**, 9609; (b) L. Qin, J. S. Hu, M. D. Zhang, Y. Z. Li and H. G. Zheng, *Cryst. Growth Des.*, 2012, **12**, 4911; (c) Q. Yue, L. Yan, J. Y. Zhang and E. Q. Gao, *Inorg. Chem*., 2010, **49**, 8647.
21 X. X. Wang, B. Yu, K. Van Hecke and G. H. Cui, *RSC ADV*, 2014, **4**, 61281.
22 J. H. Cavka, S. Jakobsen, U. Olsbye, N. Guillou, C. Lamberti, S. Bordiga and K. P. Lillerud, *J. Am. Chem. Soc.*, 2008**, 130**, 13850.
23 (a) H. Wang, W. T. Yang and Z. M. Sun, *Chem. Asian J*., 2013, **8**, 982; (b) M. D. Allendorf, C. A. Bauer, R. K. Bhakta and R. J. T. Houk, *Chem. Soc. Rev*., 2009, **38**, 1330.
24 (a) P. Cui, Z. Chen, D. L. Gao, B. Zhao, W. Shi and P. Cheng, *Cryst. Growth Des.*, 2010**, 10**, 4370; (b) L. L. Liang, S. B. Ren, J. Zhang, Y. Z. Li, H. B. Du and X. Z. You, *Cryst. Growth Des*., 2010**, 10**, 1307.
25 J. S. Hu, Y. J. Shang, X. Q. Yao, L. Qin, Y. Z. Li, Z. J. Guo, H. G. Zheng and Z. L. Xue, *Cryst. Growth Des*., 2010, **10**, 2676.
26 (a) L. Wen, Z. Lu, J. Lin, Z. Tian, H. Zhu and Q. Meng, *Cryst. Growth Des.*, 2007, **7**, 93; (b) L. P. Zhang, J. F. Ma, J.Yang, Y. Y. Pang and J. C. Ma, *Inorg. Chem.*, 2010, **49**, 1535; (c) L. Liu, C. Huang, Z. C. Wang, D. Q. Wu, H. W. Hou and Y. T. Fan, *CrystEngComm*, 2013, **15**, 7095.
27 D. Qin, X. Zeng, Q. Li, F. Xu, H. Song and Z. Zhang, *Chem. Commun.*, 2007, **147**,147.
28 (a) T. J. Ni, F. F. Xing, M. Shao, Y. M. Zhao, S. R. Zhu and M. X. Li, *Cryst. Growth Des.*, 2011, **11**, 2999; (b) D. Hermann, H. Emerich, R. Lepski, D. Schaniel and U. Ruschewitz, *Inorg. Chem*., 2013, **52**, 2744.
29 (a) M. Yamada and S. Y. Yonekura, *J. Phys. Chem. C.*, 2009, **113**, 21531; (b) M. Cerruti, A. Perardi, G. Cerrato, and C. Morterra, *Langmuir*, 2005, **21**, 9327.

Hydrothermal Synthesis and Structural Characterization of Metal−Organic Frameworks Based on New Tetradentate Ligands

Yue Liang, Wei-Guan Yuan, Shu-Fang Zhang, Zhan He, Junru Xue, Xia Zhang, Lin-Hai Jing, Da-Bin Qin*

Three MOFs have been hydrothermally synthesized based on two new quadridentate imidazole ligands with flexible chain and rigid functional groups. Complex $\{[Zn_2(L1)\ (tp)(formate)_2]\cdot H_2O\}_n$ (**1**) is a 3D framework with 2-fold interpenetrated form which exhibits a 2-nodal (3,4)-connected **fsh**-3,4-$P2_1/c$ net with a $\{8^3\}_2\{8^5.10\}$ topology. The 3D Complex $\{[Cd_2(L2)(ip)_2]\cdot 2H_2O\}_n$ (**2**) represents the first MOFs with a (4,8)-connected **sqc22** net. Complex **3** exhibits a distinctive 2D interlocked (4,4)-connected **4,4 L28** net with the point symbol of $\{4.6^4.8\}_2\{4^2.6^4\}$.